

See discussions, stats, and author profiles for this publication at: <https://www.researchgate.net/publication/230596366>

Synthesis and Characterization of Silica-Coated Iron Oxide Nanoparticles in Microemulsion: The Effect of Nonionic Surfactants

ARTICLE in LANGMUIR · MAY 2001

Impact Factor: 4.46 · DOI: 10.1021/la0008636

CITATIONS

476

READS

880

6 AUTHORS, INCLUDING:



[Swadeshmukul Santra](#)

University of Central Florida

89 PUBLICATIONS 4,573 CITATIONS

SEE PROFILE



[Jon Dobson](#)

University of Florida

164 PUBLICATIONS 8,105 CITATIONS

SEE PROFILE



[A. F. Hebard](#)

University of Florida

382 PUBLICATIONS 16,080 CITATIONS

SEE PROFILE



[Weihong Tan](#)

University of Florida

573 PUBLICATIONS 28,029 CITATIONS

SEE PROFILE

Synthesis and Characterization of Silica-Coated Iron Oxide Nanoparticles in Microemulsion: The Effect of Nonionic Surfactants

Swadeshmukul Santra,[†] Rovelyn Tapeç,[†] Nikoleta Theodoropoulou,[§] Jon Dobson,[†] Arthur Hebard,[§] and Weihong Tan^{*,†,‡}

Department of Chemistry, McKnight Brain Institute, and Department of Physics,
The University of Florida, Gainesville, Florida 32611-7200

Received June 20, 2000. In Final Form: September 27, 2000

A water-in-oil microemulsion method has been applied for the preparation of silica-coated iron oxide nanoparticles. Three different nonionic surfactants (Triton X-100, Igepal CO-520, and Brij-97) have been used for the preparation of microemulsions, and their effects on the particle size, crystallinity, and the magnetic properties have been studied. The iron oxide nanoparticles are formed by the coprecipitation reaction of ferrous and ferric salts with inorganic bases. A strong base, NaOH, and a comparatively mild base, NH₄OH, have been used in each surfactant to observe whether the basicity has some influence on the crystallization process during particle formation. Transmission electron microscopy, X-ray electron diffraction, and superconducting quantum interference device magnetometry have been employed to study both uncoated and silica-coated iron oxide nanoparticles. All these particles show magnetic behavior close to that of superparamagnetic materials. By use of this method, magnetic nanoparticles as small as 1–2 nm and of very uniform size (percentage standard deviation is less than 10%) have been synthesized. A uniform silica coating as thin as 1 nm encapsulating the bare nanoparticles is formed by the base-catalyzed hydrolysis and the polymerization reaction of tetraethyl orthosilicate in microemulsion. All experimental results are also compared with those for particles synthesized in pure water.

Introduction

The synthesis of ultrasmall magnetic nanoparticles with uniform size distribution is very important because of their wide applications in biology and medicine,^{1–9} for example, magnetic resonance imaging (MRI) contrast agent,^{5,6,9} magnetic separation of oligonucleotides,⁷ cells, and other biocomponents,⁷ magnetically guided site specific drug delivery systems,^{3,4} and so forth. The industrial application of magnetic materials covers a broad range.^{10–15} The

strongly magnetizable fluids find numerous applications,^{10,13–15} for example, magnetic seals in motors and devices such as gas lasers, blowers, and so forth, lubricants and bearings in magnetic disk drive spindles, optical memory devices, magnetic inks for bank checks, magnetic refrigeration units, and an efficient material for magnetic recording media. Therefore, the synthesis of stable magnetic fluids containing uniformly small particles with higher saturation magnetization is very important. Pure magnetic particles themselves may not be very useful in practical applications because of the following limitations: (i) they tend to form large aggregates, (ii) their original structure may get changed if they are not stable enough resulting in the alteration of magnetic properties, and (iii) they can undergo rapid biodegradation when they are directly exposed to the biological system. Therefore, a suitable coating is very necessary to prevent such limitations. To make a stable suspension of particles for practical applications, their dimension should be sufficiently small so that precipitation due to gravitational forces could be avoided. To achieve this, particles should be made very uniform and ultrasmall (<5 nm in diameter). The basic need is, therefore, to synthesize ultrasmall, coated, and uniform particles having strong magnetic properties for their practical applications.

The water-in-oil (W/O) microemulsion has been widely used to synthesize uniform size nanoparticles of various kinds,^{16–19} including magnetic materials,^{20–24} and has become a powerful tool. This is an isotropic and thermo-

* To whom correspondence should be addressed. Phone: 352-846-2410. Fax: 352-846-2410. E-mail: tan@chem.ufl.edu.

[†] Department of Chemistry.

[‡] McKnight Brain Institute.

[§] Department of Physics.

(1) Tchikov, V.; Schutze, S.; Kronke, M. K. *J. Magn. Magn. Mater.* **1999**, *194*, 242.

(2) Winotomorbach, S.; Mullerhutholtz, W. *Eur. J. Pharm. Biopharm.* **1995**, *41*, 55.

(3) Truchaud, A.; Capolaghi, B.; Yvert, J. P.; Gourmelin, Y.; Glikmanas, G.; Bogard, M. *Pure Appl. Chem.* **1991**, *63*, 1123.

(4) Fukushima, T.; Sekizawa, K.; Jin, Y.; Yamaya, M.; Sasaki, H.; Takishima, T. *Am. J. Physiol.* **1993**, *265*, L67.

(5) Babes, L.; Denizot, B.; Tanguy, G.; Le Jeune, J. J.; Jallet, P. *J. Colloid Interface Sci.* **1999**, *212*, 474.

(6) Bengel, H. H.; Palmacci, S.; Rogers, J.; Jung, C. W.; Crenshaw, J.; Josephson, L. *Magn. Reson. Imaging* **1994**, *12*, 433.

(7) DYNALogue, News and Views from Dynal Bioscience **2000**, Issue 1 (<http://www.dynal.net>).

(8) Kemshead, J. T.; Treleaven, J. G.; Gibson, F. M.; Ugelstad, J.; Rembaum, A.; Philip, T. *Prog. Exp. Tumor Res.* **1985**, *29*, 249.

(9) Pouliquen, D.; Perroud, H.; Calza, F.; Jallet, P.; Le Jeune, J. J. *Magn. Reson. Med.* **1992**, *24*, 75.

(10) Kruis, F. E.; Fissan, H.; Peled, A. *J. Aerosol Sci.* **1998**, *29*, 511.

(11) Cao, X.; Prozorov, R.; Koltypin, Y.; Kataby, G.; Felner, I.; Gedanken, A. *J. Mater. Res.* **1997**, *12*, 402.

(12) Suslick, K.; Choe, S.; Cichowlas, A.; Grinstaff, M. W. *Nature* **1991**, *353*, 414.

(13) Berkovsky, B. M.; Medvedev, V. F.; Krokov, M. S. *Magnetic Fluids: Engineering Applications*; Oxford University Press: Oxford, 1993.

(14) Cornell, R. M.; Schwertmann, U. *The Iron Oxide. Structure, Properties, Reactions, Occurrence and Uses*; VCH: Weinheim, 1996.

(15) Raj, K.; Moskowitz, R. *J. Magn. Magn. Mater.* **1990**, *85*, 233.

(16) Li, T.; Moon, J.; Morrone, A. A.; Mecholsky, J. J.; Talham, D. R.; Adair, J. H. *Langmuir* **1999**, *15*, 4328. Stathatos, E.; Lianos, P.; DelMonte, F.; Levy, D.; Tsiourvas, D. *Langmuir* **1997**, *13*, 4295.

(17) Shiojiri, S.; Hirai, T.; Komasa, I. *Chem. Commun.* **1998**, *14*, 1439.

(18) Shah, D. O. *Micelles, Microemulsions, and Monolayers-Science and Technology*; Marcel Dekker Inc.: New York, 1998; p 19.

(19) Chang, S.-Y.; Liu, L.; Asher, S. A. *J. Am. Chem. Soc.* **1994**, *116*, 6739, 6745.

Table 1. Microemulsion Composition for the Preparation of Magnetic Nanoparticles

micro-emulsion	surfactant	solvent (oil)	cosurfactant	water (nitrogen purged)	FeCl ₃ (0.15 M)	FeCl ₂ (0.1 M)	NaOH (2.0 M)	NH ₄ OH (28–30 wt %)	TEOS (neat)
B97	Brij-97	cyclohexane							
ME1	3.5 g	45.6 mL		284.8 μ L	300 μ L	300 μ L			10 μ L
ME2	2.8 g	36.5 mL		354.0 μ L			354 μ L	354 μ L	10 μ L
I520	Igepal CO-520	<i>n</i> -heptane							
ME1	7.6 g	20.0 mL		2.6 mL	500 μ L	500 μ L			10 μ L
ME2	7.6 g	20.0 mL		2.6 mL			1.0 mL	1.0 mL	10 μ L
T100	Triton X-100	cyclohexane	<i>n</i> -hexanol						
ME1	5.3 mL	22.5 mL	5.4 mL	620 μ L	500 μ L	500 μ L			10 μ L
ME2	5.3 mL	22.5 mL	5.4 mL	810 μ L			810 μ L	810 μ L	10 μ L

dynamically stable single-phase system that consists of three components: water, oil, and an amphiphilic molecule, called surfactant. The surfactant molecule lowers the interfacial tension between water and oil resulting in the formation of a transparent solution. The water nanodroplets present in the bulk oil phase serve as a nanoreactor for the synthesis of nanoparticles of different kind of materials. The shape of the water pool is spherical. The size of the water pool greatly influences the size of the nanoparticles. Thus, the size of the spherical nanoparticles can be controlled and tuned by changing the size of the water pool (W_0 value, the water-to-surfactant molar ratio). In general, the higher the value of W_0 , the larger the particle size.

In an effort to make ultrasmall, coated, and uniform size magnetic nanoparticles, we present here W/O microemulsion mediated sonochemical synthesis^{11,12} of superparamagnetic iron oxide nanoparticles in nonionic surfactants using two different inorganic bases. These nanoparticles are also coated with a thin layer of silica^{25–27} to protect the core. Particles so obtained have diameters as small as 1–2 nm, and the thickness of the silica coating is as thin as 1–2 nm. Three different types of nonionic surfactants (Brij-97, Triton X-100, and Igepal CO-520) are used for the preparation of microemulsions, and we have certainly observed the difference with respect to particle size and magnetic properties. The effect of surfactants on the particle size and uniformity is discussed in detail for both coated and uncoated particles. Following the microemulsion route, iron oxide nanoparticles are synthesized first by the coprecipitation of iron salts (ferrous and ferric) with the inorganic base (aqueous NaOH or NH₄OH solution). The effect of two different basic solutions on the particle formation is also discussed. The addition of tetraethyl orthosilicate (TEOS) directly to the microemulsion containing excess base undergoes hydrolysis and polymerization reaction.^{28,29} This reaction rate is much slower in microemulsion in comparison to the bulk aqueous solution. Therefore, with time, as the polymerization reaction goes on, a thin layer of uniform silica coating is formed surrounding each nanoparticle. This coating

protects the core magnetite nanoparticles from possible degradation influenced by the outside environment. The outer silica surface is biocompatible and functionalizable. The surface chemistry of the silica surface is simple and can be modified in various ways. To protect agglomeration of particles, the silica surface can be covalently modified into a neutral or charged surface.

Materials and Methods

Chemicals were purchased from commercial sources. They were reagent grade of high purity and used as received. Ferric(III) chloride, ferrous(II) sulfate, *n*-hexane, Triton X-100 {polyoxyethylene(10)isooctylphenyl ether, 4-(C₈H₁₇)C₆H₄(OCH₂CH₂)_{*n*}OH, *n* ~ 10}, Brij-97 {polyoxyethylene(10)oleyl ether, C₁₈H₃₅(OCH₂CH₂)_{*n*}OH, *n* ~ 10}, Igepal CO-520 {polyoxyethylene(5)nonylphenyl ether, 4-(C₉H₁₉)C₆H₄(OCH₂CH₂)_{*n*}OH, *n* ~ 5}, and tetraethyl orthosilicate were purchased from Aldrich Chemical Co. Inc. (Milwaukee, WI). Cyclohexane, *n*-heptane, *n*-hexanol, sodium hydroxide, and ammonium hydroxide (28–30 wt %) were obtained from Fischer Scientific Co. (Pittsburgh, PA). Distilled deionized water (EasyPure) was used for the preparation of all aqueous solutions.

The ultrasonicator used for the synthesis of nanoparticles was purchased from Fischer Scientific Co. (model number FS20).

Transmission Electron Microscopy (TEM). Particle size has been characterized by a Hitachi H-7000 microscope (Japan). The maximum resolution of the instrument was 0.2 nm. TEM samples were prepared by placing a drop of microemulsion containing nanoparticles directly onto the carbon-coated copper grids. These grids were kept over Kimwipes EX-L tissue papers to absorb excess microemulsion solution and then air-dried at room temperature at least for 2 days before taking images.

X-ray Electron Diffraction (XRD). The structure of the powder samples was measured using a Philips Electronic Instruments APD 3720 X-ray diffractometer. The X-ray diffraction patterns were taken from 10 to 80° (2θ value) using Cu K α radiation with an intensity ratio (α_2/α_1) = 0.5 and wavelengths of 1.54439 and 1.54056 Å, respectively.

Superconducting Quantum Interference Device (SQUID) Magnetometry. The magnetic properties of the nanoparticles were studied by a SQUID magnetometer (Quantum Design MPMS-5S). About 10 mg of sample in powder form was inserted in a gelatin capsule for the magnetic measurement at room temperature. Plots of magnetic moment versus applied magnetic field were obtained directly from the instrument. Field strength was varied in the range from –2.0 to 0.0 and 0.0 to +2.0 T (1 T = 10 000 Oe) in each scan. Magnetic moment values were calibrated in terms of emu/g.

Synthesis of Nanoparticles. Two separate microemulsions (ME1 and ME2) were prepared using each surfactant (see Table 1). The abbreviated terms B97, I520, and T100 refer to Brij-97, Igepal CO-520, and Triton X-100 surfactant containing microemulsions, respectively. ME1 contained the iron salts, FeSO₄ and FeCl₃, whereas ME2 had the base, either NaOH or NH₄OH. All aqueous solutions were prepared with deoxygenated water (nitrogen purged). The microemulsion is then placed in an ultrasonicator with magnetic stirrer removed. ME2 was then added dropwise to ME1 using a glass syringe. Upon mixing the two microemulsions, the water droplets collide and coalesce, allowing the mixing of the reactants to produce the nanoparticle.^{16–19} The formation of magnetic nanoparticles was

(20) Lopez Perez, J. A.; Lopez Quintela, M. A.; Mira, J.; Rivas, J.; Charles, S. W. *J. Phys. Chem. B* **1997**, *101*, 8045.

(21) Lopez Perez, J. A.; Lopez Quintela, M. A.; Mira, J.; Rivas, J. *IEEE Trans. Magn.* **1997**, *33*, 4359.

(22) Dresco, P. A.; Zaitsev, V. S.; Gambino, R. J.; Chu, B. *Langmuir* **1999**, *15*, 1945.

(23) Lee, K. M.; Sorensen, C. M.; Klabunde, K. J.; Hadjipanayis, G. C. *IEEE Trans. Magn.* **1992**, *28*, 3180.

(24) Liu, C.; Zou, B.; Rondinone, A. J.; Zhang, Z. J. *J. Phys. Chem. B* **2000**, *104*, 1141.

(25) Atarashi, T.; Kim, Y. S.; Fujita, T.; Nakatsuka, K. *J. Magn. Mater.* **1999**, *201*, 7.

(26) Wang, G.; Harrison, A. J. *Colloid Interface Sci.* **1999**, *217*, 203.

(27) Ohmori, M.; Matijevic, E. *J. Colloid Interface Sci.* **1992**, *150*, 594.

(28) Stober, W.; Fink, A. J. *Colloid Interface Sci.* **1968**, *26*, 62.

(29) Arriagada, F. J.; Osseo-Asare, K. *J. Colloid Interface Sci.* **1999**, *211*, 210.

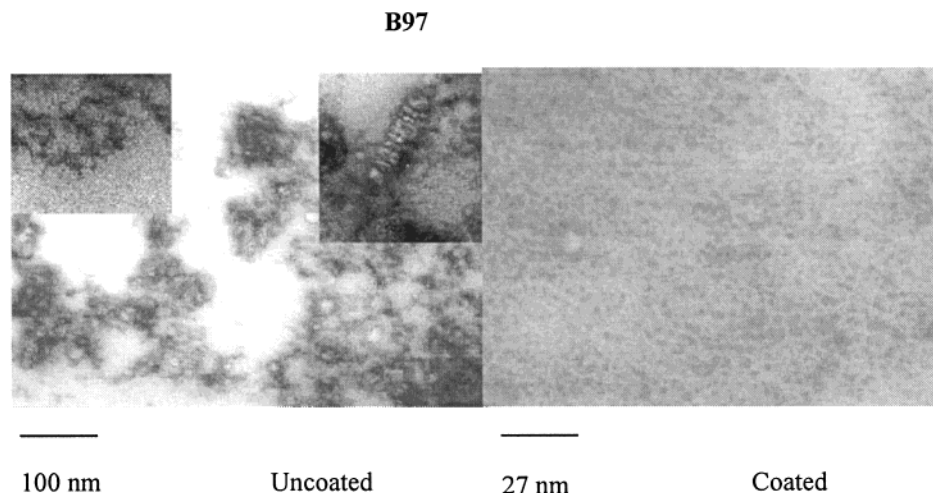


Figure 1. TEM images of uncoated (left panel) and coated (right panel) magnetic nanoparticles prepared in Brij-B97 using NaOH. Insets show the hyperbranched and acicular structures.

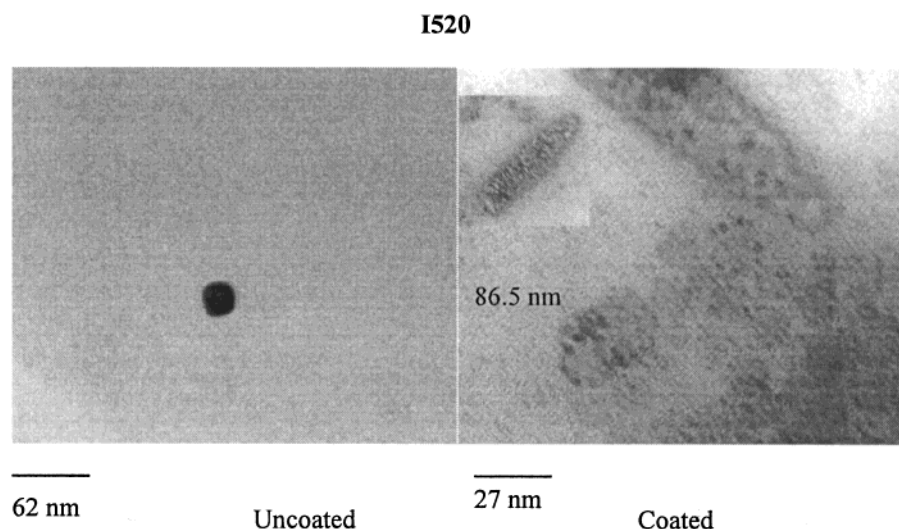


Figure 2. TEM images of uncoated (left panel) and coated (right panel) magnetic nanoparticles prepared in Igepal CO-520 using NaOH.

visually realized by the appearance of a deep brown color of the microemulsion mixture.^{20–24} Nitrogen gas was continuously purged during mixing and sonication when NaOH is used as a base. The resulting microemulsion was further sonicated for 2 h. The resultant fluid was then flocculated and washed several times with sufficient amount of ethanol (95%) and centrifuged. For each washing, the sonicator is used to completely disperse the nanoparticles in ethanol. Surfactant molecules were almost completely removed during this process. Pure nanoparticles could then be collected either by magnetic separation directly from ethanolic dispersion or by centrifugation. The size of the particles formed is mechanically limited by the size of the water droplets, which is determined by the structure and the concentration of the components. Silica-coated particles were prepared in a similar manner as the uncoated one with the exception that ME2 contained neat TEOS (Table 1). The base-catalyzed hydrolysis of TEOS produces silicic acid, which undergoes polymerization reaction and finally forms the silica coating.^{28,29} ME2 was allowed to stir for an hour before it was added to ME1. Resultant silica-coated magnetic nanoparticles were isolated after 24 h of aging. In the present study, the value of W_0 was kept constant at 10 for all microemulsions. At a lower value of W_0 , magnetic nanoparticles did not form a clear suspension in microemulsion. They tend to aggregate and precipitate out of the microemulsion before they are treated for silica coating.

With Brij-97, both microemulsion ME1 and ME2 were heated to 65 °C in a water bath while stirring magnetically until a uniform single-phase solution resulted. Both ME1 and ME2 became cloudy upon addition of iron salts and base, respectively.

A complete transparent brown solution resulted when they were combined together at a hot condition (65 °C). Upon cooling, phase separation occurred with an appearance of a brown layer on top. This brown layer containing nanoparticles was collected by a separating funnel. With Igepal CO-520 and Triton X-100, a transparent single-phase microemulsion always resulted at room temperature. For comparison, we have also made particles in deoxygenated pure water (bulk) using NaOH as a base.

Results

Characterization of Magnetic Nanoparticles. TEM Measurements. TEM images of both uncoated and silica-coated particles are shown in Figures 1, 2, and 3 for B97, I520, and T100, respectively. Figure 4 shows the particles prepared in bulk water. Most of the particles are aggregated, and therefore the determination of actual particle size becomes difficult.

In Brij-97 (Figure 1), uncoated particles shown on the left panel are aggregated in two different fashions: hyperbranched and acicular (ellipsoidal)-shaped structures irrespective of the nature of the base used (see inset, left panel). The size of individual particles is about 1–2 nm (ultrasmall, Table 2). Because of their ultrasmall size, we could not measure precisely the actual diameter of each particle and hence the particle size distribution. An approximate measurement of the size distribution is done

T100

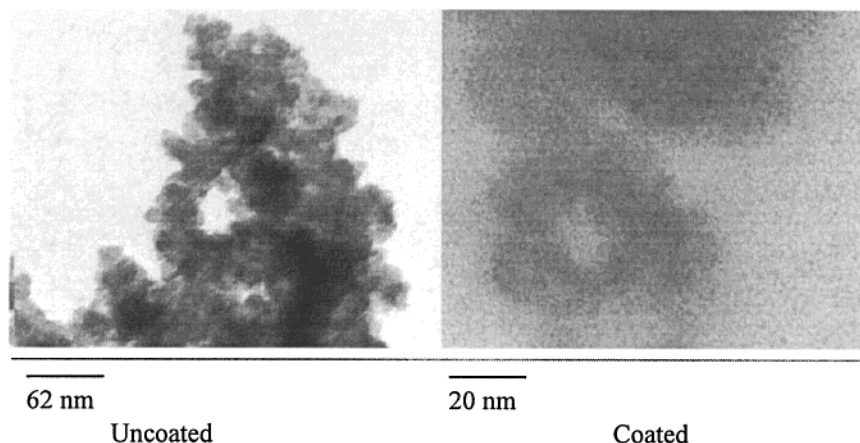


Figure 3. TEM images of uncoated (left panel) and coated (right panel) magnetic nanoparticles prepared in Triton X-100 using NaOH.



Figure 4. TEM image of bulk magnetic particles.

manually with the help of Digital Micrograph software associated with the Gatan 792 Bioscan digital camera. The camera was equipped with the TEM instrument. The percentage standard deviation is found to be less than 10% (uniform). The formation of a hyperbranched structure is associated with the wirelike "head-to-tail" alignment of the magnetic particles. In the acicular-shaped structure, particles are not densely packed; rather, they are arranged in such a way to create uniform pores. They can be better identified as sieves (Figure 1, left panel). Some acicular-shaped aggregations consist of uniformly spaced parallel layers of particles along the minor axis. These structural features get completely lost when they are coated with the silica (Figure 1, right panel). Monodisperse silica-coated particles of very uniform size (3–4 nm) are obtained when NaOH is used as a base. In NH_4OH , coated particles of uniform size (3–4 nm) tend to aggregate further to form a spherical structure as if magnetic nanoparticles are doped inside the silica network.

In Igepal CO-520 (Figure 2), particles are found to be less aggregated when NH_4OH is used. Their size ranges between 4 and 5 nm (Table 2), and interestingly, when they are coated with silica the particles aggregate to form tubule structures as long as 350 nm. The diameter of these nanotubes is very uniform (about 25 nm). When NaOH

Table 2. Data Obtained from TEM, XRD, and SQUID

sample	TEM (particle size in nm)	XRD (peak broadness in nm)	SQUID specific magnetization (emu/g)	
			10 KOe	20 KOe
bulk (uncoated)		9 ± 4	14.6	18.3
		B97		
NaOH coated	3 ± 1		0.212	0.311
NaOH uncoated	2 ± 1	27 ± 4	0.540	0.896
NH_4OH coated	3 ± 1			
NH_4OH uncoated	2 ± 1	40 ± 4		
		I520		
NaOH coated	4 ± 1		0.352	0.688
NaOH uncoated	2 ± 1		0.650	1.190
NH_4OH coated	9 ± 4		0.246	0.474
NH_4OH uncoated	4 ± 2		0.437	0.852
		T100		
NaOH coated	3 ± 1		0.286	0.555
NaOH uncoated	2 ± 1	22 ± 4	0.636	1.22
NH_4OH coated	6 ± 1			
NH_4OH uncoated	4 ± 1	21 ± 4		

is used, aggregated particles so obtained are mostly spherical composed of many small particles of 2–3 nm size. The typical size of spheres is 22 ± 3 nm (Figure 2, left panel). When they are coated with silica, aggregated particles still retain their spherical shape with a very thin layer (1–2 nm) of coating and they remain well dispersed. Additionally, the formation of acicular-shaped aggregation, as long as 400 nm, is also seen (Figure 2, right panel). The pattern of the interior of the acicular-shaped structure is observed to be very similar to that obtained in Brij-97.

In Triton X-100 (Figure 3), particles are again very uniform and small but they are aggregated (Table 2). The aggregation pattern in NH_4OH is similar to that obtained in Brij-97. However, no acicular-shaped structures are seen; rather, about 10% of particles are observed to be aggregated in a nonuniform and compact spherical fashion. Particles synthesized using NaOH have a spongelike porous structure (Figure 3, left panel) that consists of small particles of about 1–2 nm size. The aggregation pattern in Triton X-100 does not change when particles are silica-coated. Particles synthesized in pure deoxygenated water show extremely nonuniform, irregular shapes. They are mostly obtained in the form of large aggregates, as expected (Figure 4).

XRD Measurement. X-ray diffraction spectra of uncoated and coated particles synthesized in microemulsions are shown in Figure 5a–f. They are compared with the same

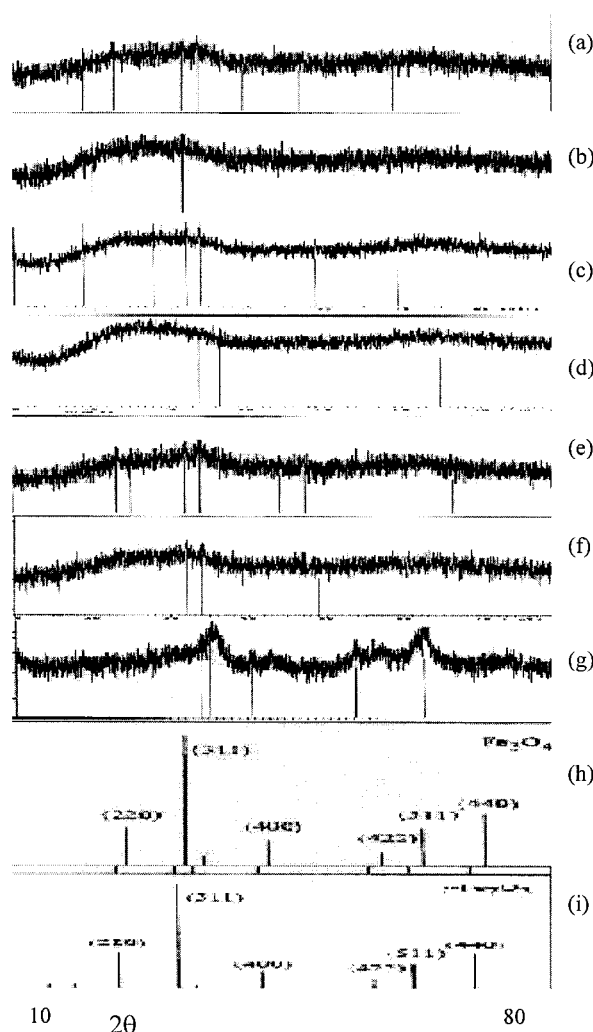


Figure 5. XRD diffractograms for particles prepared in (a) bulk, (b) Brij-97 using NaOH, (c) Brij-97 using NH_4OH , (d) Triton X-100 using NaOH, (e) Triton X-100 using NH_4OH , (f) Igepal CO-520 using NaOH, and (g) Igepal CO-520 using NH_4OH . Standard diffractograms for (h) Fe_3O_4 and (i) $\gamma\text{-Fe}_2\text{O}_3$.

material prepared in the bulk water phase (Figure 5g). From Figure 5, it is clearly seen that particles synthesized from the microemulsions do not show sharp diffraction peaks corresponding to extended crystalline structure. Instead, a broad band appears in each spectrum. This observation is typical for amorphous materials and also for ultrasmall crystalline materials where diffraction peaks cannot be well resolved. Although our bulk sample also does not show any sharp peak, still, diffraction peaks can be resolved. The diffraction pattern of our bulk magnetic sample is close to the standard pattern for crystalline magnetite (Fe_3O_4) or maghemite ($\gamma\text{-Fe}_2\text{O}_3$) or a mixture of both (Figure 5h,i). Our experimental data cannot clearly distinguish between these two types of iron oxides. Because they have very similar magnetic properties, the identification is not important in the present study. We have approximately calculated the relative broadness of the most intense diffraction peak (main diffraction line of the standard sample for magnetite, 311 peak) of the spectra for both coated and uncoated samples synthesized in microemulsions and compared with the bulk sample (See Table 2). The maximum broadness appears for the uncoated particles synthesized in Brij-97 using NH_4OH , and the minimum appears in the bulk sample.

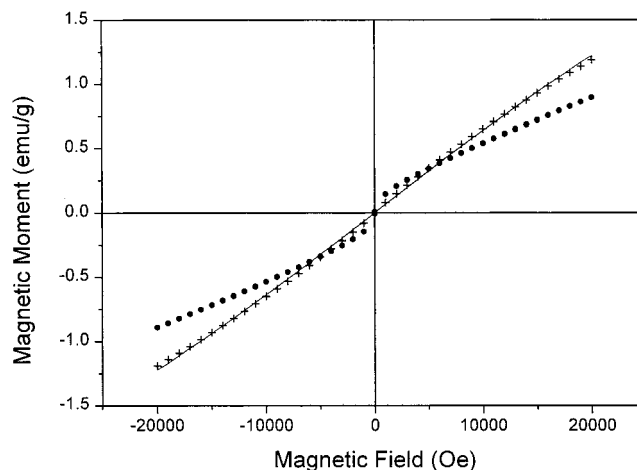


Figure 6. Magnetization curve for uncoated particles prepared in microemulsions using Brij-97 (●), Igepal Co-520 (+), and Triton X-100 (solid line).

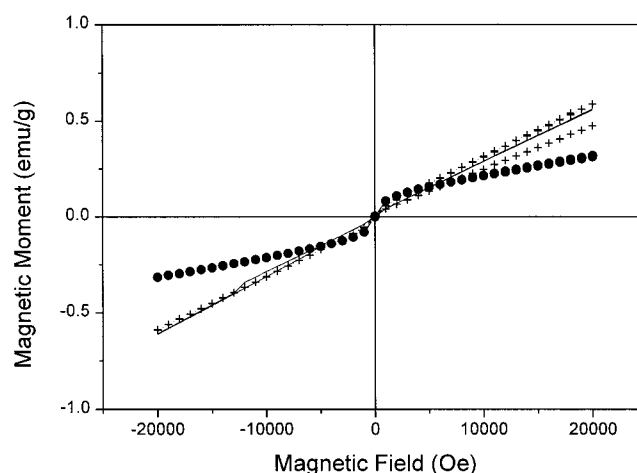


Figure 7. Magnetization curve for coated particles prepared in microemulsions using Brij-97 (●), Igepal CO-520 (+), and Triton X-100 (solid line).

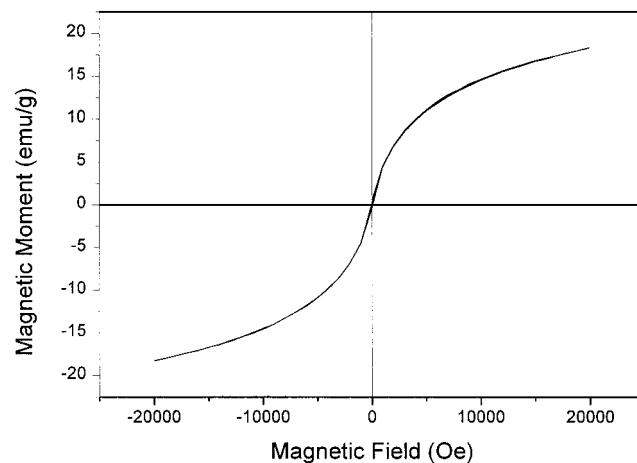


Figure 8. Magnetization curve for bulk material.

SQUID Measurement. The field and specific magnetization (magnetic moment per gram) at two values of the external magnetic field (10 and 20 kOe) are compiled in Table 2 for particles synthesized in microemulsions as well as in bulk water. Room-temperature magnetization curves are shown in Figures 6 and 7 for uncoated and silica-coated particles, respectively. Figure 8 shows the magnetization curve for the bulk sample. The applied

magnetic fields are not corrected for demagnetization effects. Results thus obtained from SQUID magnetometric measurement show a very good correlation with those of TEM and XRD measurements (see discussion section). At room temperature, saturation of magnetization is not observed when the applied field is increased up to the value of 20 KOe for all samples. At any given field, the magnetization for the uncoated sample is always higher than that of the coated sample. As expected, a much higher value of magnetization (about 25 times at 10 KOe) is observed for the bulk sample when compared with the samples synthesized via the microemulsion route. The shape of the magnetization curves for the coated particles are very similar, exhibiting a "knee" near 1.2 KOe where there is a crossover from easy to hard moment relaxation. For the uncoated particles, a similar knee is observed only for the Brij-97 sample whereas Igepal CO-520 and Triton X-100 showed a linear behavior. The magnetization for the bulk sample becomes relatively flat at 20 KOe with a magnetization a factor of 4 less than the saturation magnetization of pure Fe_3O_4 . The behavior of the coated particle synthesized in Brij-97 is close to that of the bulk sample.

Discussion

The water-in-oil microemulsion has been prepared using nonionic surfactants. The water nanodroplets (nanoreactor) containing reagents undergo rapid coalescence that allows mixing, precipitation reaction, and aggregation processes for the synthesis of magnetic nanoparticles. The nanoreactor water pool is spherical in shape, and surfactant molecules surround the nanodroplet wall. These walls act as cages for the growing particles and thereby reduce the average size of the particles during the collision and aggregation process. In the present study, we have observed very clearly that nonionic surfactants affect the particle size and the aggregation process.

We believe that the formation of particles is first accompanied by a very fast precipitation reaction and aggregation process. The nascent particles so formed are spherical in shape. They are very uniform (percentage standard deviation is less than 10%) and ultrasmall (<5 nm in diameter) as shown in TEM images in Figures 1, 2, and 3 and also from TEM data compiled in Table 2. In the next step, interparticle collisions occur under the influence of ultrasonication which leads to agglomeration, changing the morphology of the particles.³⁰ This agglomeration process facilitates the preferential adsorption of the surfactant molecules onto the particle's surface. Nonionic surfactants consist of polyoxyethylene moiety with a terminal hydroxyl group as a polar part and a long hydrocarbon chain as a tail part. It is thus very reasonable that the terminal hydroxyl group will interact by a weak hydrogen bonding force with the oxygen atoms present on the particle surface. The tail part, thus, will be away from the particle surface. The preferential surfactant adsorption restricts the sideways interconnection of the particles and allows a further aggregation process in an ordered fashion. During this process, hydrophobic tails of the surfactants remain parallel and interact with each other to stabilize the system and finally acicular particles are formed. Depending on the chemical structure of the surfactant molecules, the extent of surfactant molecule adsorption onto the surface of the nanoparticle varies. From the structures of the nonionic surfactants (see materials and methods section), it appears very clear that the Brij 97 surfactant has a longer hydrophobic chain (oleyl group)

when compared to Igepal CO-520 (nonylphenyl group) and Triton X-100 (isooctylphenyl group). It is, therefore, expected that there will be a strong hydrophobic-hydrophobic interaction between oleyl groups attached to adjacent nanoparticles. This could be the reason we have observed a more ordered fashion in particle aggregation in the case of Brij 97 when compared to the other surfactants. When coated with silica, the extent of surfactant molecule adsorption onto the silica surface is less compared to the bare particles resulting in the formation of more discrete particles. Also, the ultrasound radiation generated from the ultrasonicator affects the adsorption process. This could be the reason particles synthesized using different surfactants had different morphologies. The formation of spherical particles occurs at the very first step of aggregation. Depending on the nature of surfactant molecules and their adsorption capabilities, individual spherical particles can further aggregate to form tubelike structures. We have observed this phenomenon in Igepal CO-520 during the silica coating process with NaOH. The hydrolysis and polymerization reaction by NH_4OH generally forms stable spherical particles;²⁹ that too we have observed in Igepal CO-520. The magnetic dipole-dipole interaction sometimes also plays an important role in forming elongated particles.³¹ In addition, the use of strong base for the precipitation reaction of iron salts can also affect the particle morphology.

In the presence of a large amount of strong base, the total ionic strength of the water pool increases. This causes instability of the microemulsion system. To avoid this problem, we used a very small amount of base which was sufficient for the precipitation reaction followed by the polymerization reaction of TEOS (silica-coated, Stober's synthesis).^{28,29} We did not observe any major difference in particle morphology using strong base and mild base. TEM results compiled in Table 2 clearly show that the present method has certainly produced very uniform and ultrasmall magnetic particles with and without silica coating.

The absence of sharp peaks in the X-ray electron diffraction spectra (Figure 5) does not necessarily mean that magnetite particles so prepared by the microemulsion method are all amorphous. It is well-known that the broadness of the peak increases with the decrease in the particle size.²⁰ Therefore, they might be crystalline, but for their ultrasmall size, diffraction peaks are not well-defined. Table 2 shows that there exists a good correlation between the particle size (TEM data) and the peak broadening (XRD data). The maximum broadness appears for the uncoated particles synthesized in Brij-97 using NH_4OH , which agrees with our TEM results that particles are made very small (1–2 nm). The magnetic particles prepared in the bulk water phase did not show very sharp peaks confirming that particles are poorly crystalline.

The magnetization of ferromagnetic materials is very sensitive to the size and structure of the sample. If a sample consists of small particles, its magnetization decreases with the particle size when compared to the large particles at a certain applied field. This is due to increasing dispersion on the exchange integral that causes small particles to finally reach a superparamagnetic state with reduced exchange interaction between the particles.^{32,33} It is also known that below some critical size (<10 nm) magnetic particles become single domain because of the

(30) Doktycz, S. J.; Suslick, K. S. *Science* **1990**, *247*, 1067.

(31) Luo, W.; Nagel, S. R.; Rosenbaum, T. F.; Rosenseig, R. E. *Phys. Rev. Lett.* **1991**, *67*, 2721.

(32) Elliot, S. R. *Physics of Amorphous Materials*; Longman: London and New York, 1984; pp 350–357.

(33) Morup, S.; Trone, E. *Phys. Rev. Lett.* **1994**, *72*, 3278.

interplay between the energy of dipole fields and domain wall creation.^{14,34–36}

The presence of silica coating has been confirmed by the fluorescamine assay test³⁷ (results not shown). Also, the decrease in the magnetization (Table 2) when particles are coated with silica clearly distinguishes coated and uncoated particles. This silica coating protects the magnetic particles from possible decomposition induced by the surrounding environment, prevents further aggregation, and reduces interparticle magnetic cross talk retaining the magnetic property of each particle intact. Moreover, the silica surface can be functionalized using a variety of known surface chemistry.^{38,39}

We have successfully attached DNA molecules onto our magnetic nanoparticles.⁴⁰ The magnetic nanoparticles have been used in preliminary biomolecule immobilization studies. Ultrasmall and uniform silica-coated magnetic nanoparticles were first treated with (3-mercaptopropyl) trimethoxysilane. The mercaptosilane-activated nanoparticles were then allowed to react with 5-prime disulfide-modified oligonucleotides. The attachment of oligonucleotides onto the solid support was based on the thiol/disulfide exchange reaction. This exchange reaction is specific, and there were no side reactions involving other functional groups on the nucleotides. Oligonucleotides attached by this method provided a highly efficient substrate for nucleic acid hybridization and primer extension assays. The successful attachment of disulfide-modified oligonucleotide to the nanoparticle's surface was tested by double-stranded DNA intercalator reagent ethidium bromide (EtBr) as follows. The 5-prime disulfide-modified oligonucleotide had the sequence 5'-GCG ACC ATA GCG ATT TAG A-3'. Another completely complementary oligonucleotide sequence, 5'-TCT AAA TCG CTA TGG TCG C-3', was used for the hybridization process.

The formation of the double-stranded hybrid was detected by using an intercalation reagent, EtBr. A clear fluorescence signal from the hybrid was detected. The present strategy is being employed to make useful magnetic probes for the separation of target oligonucleotides, such as cellular m-RNA.

Conclusion

In this paper, we report a robust methodology for the synthesis of both uncoated and silica-coated magnetic nanoparticles of ultrasmall (<5 nm) and very uniform size distribution. Their magnetic properties are close to those of the pure superparamagnetic materials. Therefore, they can be of potential use in power transformers, magnetic recording heads, and microwave applications. Our silica (a nonmagnetic matrix)-coated magnetic particles retain their magnetic properties intact. They might also have potential applications for magnetic sensors and new storage devices with very high density. The silica surface can also be coated with biomolecules (enzymes, antibodies, DNA, etc.) and sugars (dextran, starch, albumin, poly(ethylene glycol)) for a variety of applications.⁵ Studies on the different MRI contrast agents show that the biodistribution depends on the overall particle size, surface charge, and the nature of the coating materials.^{5,6} Our ultrasmall silica-coated particles can be easily immobilized with the antibody to deliver them into a specific target via the antibody–antigen recognition. Unlike polystyrene-based magnetic particles, our silica-coated nanoparticles can be easily dispersed in organic and aqueous solutions. These coated particles would also be very useful for efficient biomolecule separation technology, for example, DNA/RNA separation, cell separation, and so forth, and also for magnetically guided biosensor applications. We are now focusing on the biomedical applications of these magnetic nanoparticles in the above-mentioned areas.

Acknowledgment. This work is partially supported by the NIH NS39891-01 and NSF CTS-0087676 and by DOR/AFOSR MURI Grant No. F49620-96-1-0026.

LA0008636

(34) Leslie-Pelecky, D. L.; Rieke, R. D. *Chem. Mater.* **1996**, *8*, 1770.

(35) Gonsalves, K. E.; Rangarajan, S. P.; Garcia-Ruiz, A.; Law, C. C. *J. Mater. Sci. Lett.* **1998**, *15*, 1261.

(36) Kang, Y. S.; Risbud, S.; Rabolt, J. F.; Stroeve, P. *Chem. Mater.* **1996**, *8*, 2209.

(37) Chung, L. A. *Anal. Biochem.* **1997**, *248*, 195.

(38) Cordek, J.; Wang, X. W.; Tan, W. H. *Anal. Chem.* **1999**, *71*, 1529.

(39) Fang, X. H.; Liu, X. J.; Schuster, S.; Tan, W. H. *J. Am. Chem. Soc.* **1999**, *121*, 2921.

(40) Lou, H.; Lang, X.; Hillard, L.; Tan, W. *SPIE* **4264**, 59–65. Santra, S.; Wang, K.; Tapeck, R.; Tan, W. *J. Biomed. Opt.*, in press.